Nonlinear Stress-Strain Behavior of Graphite/Epoxy Laminates

Paul A. Lagace*
Massachusetts Institute of Technology, Cambridge, Massachusetts

The nonlinear stress-strain behavior of graphite/epoxy was investigated. One hundred and eighty-one coupon specimens of the $[\pm\theta]_s$ family, with θ equal to 0°, 5°, 10°, 15°, 20°, 25°, 30°, 35°, 40°, 45°, 50°, 55°, 60°, 75°, and 90°, were tested in uniaxial tension. All specimens were unnotched. Three types of tests were conducted: monotonic-to-failure; load, unload, reload-to-failure; and 100 load-unload cycles followed by a load-to-failure. In the latter two cases, the load cycle entered the nonlinear stress-strain region of the specimen. Two basic loadings were found to cause nonlinear stress-strain behavior in a unidirectional ply: longitudinal tension, which causes "stiffening," and shear, which causes "softening." These effects combined to cause overall stiffening in the $[\pm\theta]_s$ laminates for θ less than 20°, and softening for θ greater than 20°. The load, unload, reload tests showed three important results. First, there was a "permanent strain" left at zero load for those laminates that softened. Second, the reload path has the same modulus as the original load path and rejoins the basic stress-strain curve at the point to which the laminate was previously loaded. Third, the laminates show no memory of one previous loading after being reloaded to the original load point as further loading produces a stress-strain curve unaltered by one load, unload, reload cycle including no change in fracture stress. Implications for general laminates are discussed.

Nomenclature

C.V. = coefficient of variation
E_L = longitudinal modulus
E_T = transverse modulus
G_{LT} = shear modulus
Hg = mercury
θ = lamination angle
μ strain = microstrain
ν_{LT} = major Poisson's ratio

Background

THE stress-strain behavior of advanced composite materials, especially graphite/epoxy, is generally classified as linear-to-failure. For unidirectional composites loaded along the fiber direction, this is accurate to within 10 to 15%. But, as Sendeckyj[1] points out, there is some nonlinearity in the fiber modulus (increasing stiffness with increasing strain level) which will manifest itself in the stress-strain behavior of the basic unidirectional ply. In composites for which the matrix material is a 350°F cure thermosetting resin, typical of those used in the aerospace industry, the stress-strain behavior of the basic unidirectional ply when loaded perpendicular to the fiber is generally linear-to-failure. Failure occurs at relatively low (on the order of 50 MPa) stress levels before matrix nonlinearity can become important. However, when shear stresses are present, the unidirectional ply shows significant nonlinear stress-strain behavior.

With general laminates, even in the absence of applied shear loads, shear stresses are induced in the individual angled plies with respect to an axis sytem aligned with the fibers in that ply (known as ply axes). This is due to the manner in which composite laminates carry load. Analyses can be performed using classical laminated plate theory (CLPT) to calculate these ply stresses in ply axes. Thus, nonlinear stress-strain behavior can occur in a laminate under any type of applied load. The nonlinear behavior becomes more important as the design strains of composite structures are increased, especially at stress raisers such as holes.

Previous work on the nonlinear stress-strain behavior of composite laminates has concentrated on predicting this stress-strain behavior in laminates based on the measured stress-strain behavior of the basic unidirectional ply under the five monotonic-to-failure loading conditions required to characterize the ply behavior: longitudinal tension, longitudinal compression, transverse tension, transverse compression, and shear. Researchers have used various methods to model the stress-strain behavior of the unidirectional ply in conjunction with CLPT to determine the stress-strain response of general laminates. Petit and Waddoups[2] used an incremental approach with the experimental stress-strain curves of the unidirectional ply modeled as piecewise linear. Some authors have assumed that only the shear stress-strain response is nonlinear and have then modeled this relationship as cubic in stress,[3,4] or used a piecewise linear representation of the shear relationship[5] with linear relationships for the other four loading conditions. Foye[6,7] used the finite element method with constant strain triangles and the basic stress-strain behavior of the fiber and matrix to get a stress-strain curve for the composite and extend this to a laminate. His results were highly dependent on the number of increments used to model the stress-strain curves. Cubic spline fits were used by Sandhu[8] to model shear and transverse stress-strain behavior with the longitudinal behavior assumed linear. Sendeckyj[1] extended this to model all the stress-strain curves with cubic spline functions. These methods have met with some success.

Much of this work in nonlinear stress-strain behavior has been inspired by strength considerations.[9] Indeed, general laminates can exhibit nonlinear stress-strain behavior due to total or partial failure of individual plies.[10,11] However, this behavior generally manifests itself by sharp discontinuities and jumps in the stress-strain curve[12] rather than a smoothly varying nonlinear behavior.

Scope of Work

The present work is an experimental look at the nonlinear stress-strain behavior of graphite/epoxy due to the basic stress-strain nonlinearity of the unidirectional ply under various loadings (analytical results will be presented in a

Received March 24, 1984; presented as Paper 84-0860 at the AIAA/ASME/ASCE/AHS 25th Structures, Structural Dynamics and Materials Conference, Palm Springs, CA., May 14-16, 1984; revision received Dec. 24, 1984. Copyright © American Institute of Aeronautics and Astronautics, Inc., 1985. All rights reserved.

*Assistant Professor, Aeronautics and Astronautics, Technology Laboratory for Advanced Composites. Member AIAA.

forthcoming paper). Nonlinearity due to gross initial failures was purposefully not considered since it is a distinctly separate phenomenon which generally results in discontinuities in the stress-strain curve. Thus, various laminates of the $[\pm\theta]_s$ family were investigated under uniaxial load for values of θ of 0°, 5°, 10°, 15°, 20°, 25°, 30°, 35°, 40°, 45°, 50°, 55°, 60°, 75°, and 90°. Nonlinear stress-strain behavior, due to shear, is most apparent in these laminates due to the lack of fibers in direct line with a longitudinally applied load.

Basic stress-strain behavior to failure was determined for these laminates in order to ascertain the interactions of the various stress-strain nonlinearities. More important,[14] the stress-strain behavior of these laminates was examined under load, unload, reload cycles. This yielded information on hysteresis effects, effects of this cycle on moduli and failure stress, as well as the phenomenon of "permanent strain" left in a material after a load-unload cycle. Such strain may accumulate over many load cycles and lead to reduced strength of the material.

Experimental Program

A total of 181 graphite/epoxy specimens were manufactured and tested. The material used throughout the program was Hercules AS1/3501-6 graphite/epoxy unidirectional preimpregnated tape supplied in 300-mm wide rolls and stored at temperatures below 0°F. The prepreg was cut using Stanley knives and laid up with the use of a jig to assure proper fiber angles from ply to ply. The material was cured as 300×350 mm plates in an autoclave under 85 psi and 30 in. Hg vacuum in a two-step process: a 1-h hold at 240°F and a 2-h hold at 350°F, as recommended by the manufacturer. The cured plates were postcured in an oven at 350°F for 8 h. The laminates were cut into 50-mm wide strips on a milling machine with a specially designed table using a water-cooled diamond wheel. All specimens were unnotched. A pair of eight-ply glass/epoxy loading tabs made of Scotchply Type 1002 were bonded onto each end of the graphite/epoxy strip, using film adhesive FM-123-2 supplied by American Cyanamid. This process resulted in a specimen 350 mm long and 50 mm wide as depicted in Fig. 1. The tabs were 75 mm long, resulting in a test section of 200 mm.

Longitudinal strain gages were bonded onto all specimens. Strain gage type EA-09-125AD-120 manufactured by Micro Measurements was used throughout. The gage was placed at the specimen center, as shown in Fig. 1.

Eight different types of tests were conducted on the specimens, although all eight were not conducted on any one particular laminate. The entire test program is shown in Table 1. These test types are represented by three different groups. The first group, which includes only test type A, is a simple monotonic-to-failure test. The second group, comprised of test types B through F, is a load, unload, load-to-failure sequence. The point to which the specimen is originally loaded is classified in these cases as the quarter, third, half, two-thirds, and three-quarters point. This relates to the amount of stress applied to the specimen. Specifically, it is the distance, relative to the stress axis, that the specimen is loaded into the nonlinear region. The endpoints of the nonlinear region are the break stress and the failure stress, as illustrated in Fig. 2. The break stress, or break point, is defined as the point at which the specimen departs from its initial linear stress-strain behavior. In this investigation, the break stress was determined with the aid of a program developed at the Technology Laboratory for Advanced Composites known as LIN6.[13] This program determines linear regions of a data set. The third group of tests, types G and H, consists of 100 load-unload cycles to a point in the nonlinear region and then a load-to-failure. This can be summarized as follows:

A = load to failure

B = load to quarter point, unload, load to failure

C = load to third point, unload, load to failure

D = load to half point, unload, load to failure

E = load to two-thirds point, unload, load to failure

F = load to three-quarters point, unload, load to failure

G = 100 load-unload cycles to third point, load to failure

H = 100 load-unload cycles to two-thirds point, load to failure

The unload portions are to zero load.

Table 1 Experimental test program for $[\pm\theta]_s$ laminates

	Test type							
θ,°	A	B	C	D	E	F	G	H
0[a]	5[b]	—	—	5	—	—	—	—
5	3	—	3	—	3	—	3	3
10	3	—	3	—	3	—	3	3
15	3	—	3	—	3	—	3	3
20	3	—	3	—	3	—	3	3
25	5	—	—	5	—	—	—	—
30	3	5	—	5	—	5	—	—
35	3	5	—	5	—	5	—	—
40	5	—	—	5	—	—	—	—
45	5	5	—	5	—	5	—	—
50	5	—	—	5	—	—	—	—
55	5	—	—	5	—	—	—	—
60	5	—	—	—	—	—	—	—
75	5	—	—	—	—	—	—	—
90	5	—	—	—	—	—	—	—

[a]0° specimens were $[0_{12}]$, not $[0_4]$. [b]Number of specimens tested.

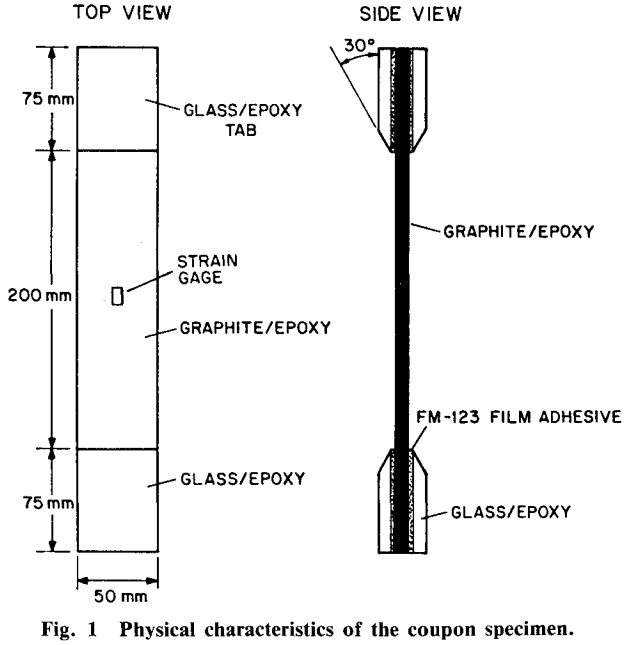

Fig. 1 Physical characteristics of the coupon specimen.

All testing was accomplished on an MTS 810 Material Test System with the aid of hydraulic grips. Specimens were first gripped in the upper grip and the load and strain readings zeroed with the specimen in this "free hanging" position. The specimen was then gripped in the bottom head and loaded at a constant stroke rate of 1 mm/min, yielding an approximate strain rate of 5000 microstrain/min. Load and strain data were recorded at 0.5-s intervals through an automated data acquisition system using a PDP-11/34 computer. Load was applied to failure for test type A and to a previously defined point for all other test types. For all but test type A, unloading was accomplished at the same stroke rate, and data continued to be taken. For test types B through F, the specimens were ungripped from the bottom head to allow the load to return to zero when the machine stroke returned to zero. Strain readings were taken at this point after several minutes. The specimens were then regripped and loaded to failure with the same stroke rate. For the cyclic tests, types G and H, the same procedure was followed except that the specimens were not ungripped at the end of each unloading.

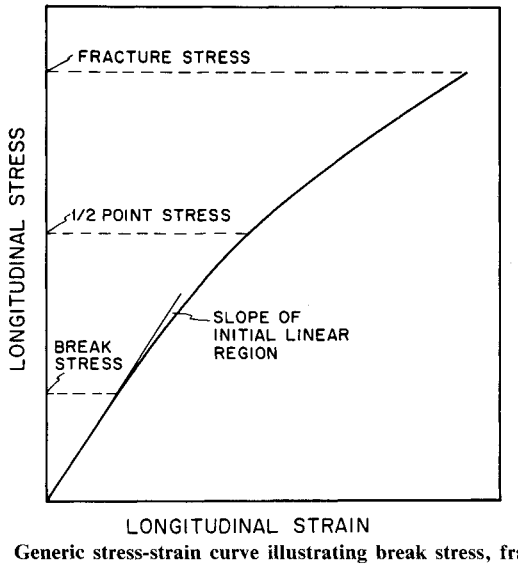

Fig. 2 Generic stress-strain curve illustrating break stress, fracture stress, and intermediate points.

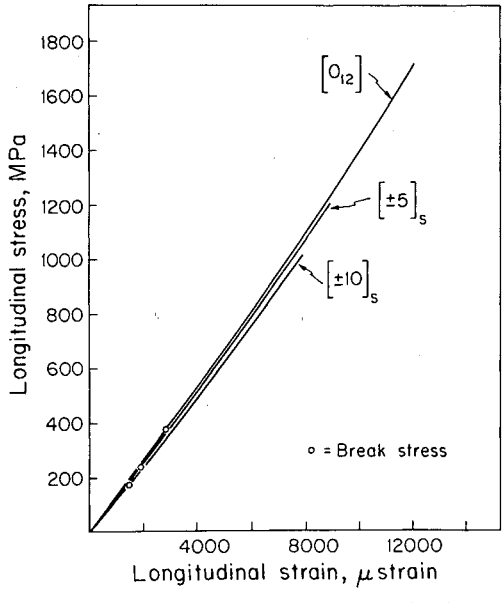

Fig. 3 Typical stress-strain behavior for $\theta = 0°$, 5°, and 10°.

Fracture loads were recorded for each specimen at the conclusion of the test. The manufacturer's nominal ply thickness of 0.134 mm was used for reduction of all loads to stresses rather than the actual measured laminate thicknesses. This allowed the data to be reduced to a common base independent of slight manufacturing variations. The average corrected measured per ply thickness of all 181 specimens is 0.136 mm with a coefficient of variation of less than 2%. Thickness measurements were taken at 9 locations on each coupon.

Results

Monotonic-to-Failure Tests

Typical stress-strain curves from the monotonic-to-failure tests are shown in Figs. 3-6. Three pieces of information are obtained from each of these curves: the break stress, the initial modulus, and the final modulus, or percentage change in modulus from beginning to end of test. In all discussions, modulus refers to tangent modulus.

The average break stresses for the monotonic tests are reported in Table 2. These stresses are determined for each specimen as described in the previous section. There is considerable variation in these stresses. The coefficient of variation is generally in the vicinity of 15%. There are, however, several notable exceptions, the most dramatic being for the $[\pm 25]_s$ specimens with a coefficient of variation of 47.2% for the break stresses. This can be attributed to the fact that these specimens are relatively linear-to-failure, as can be seen in Fig. 4. Note that the $[\pm 75]_s$ and $[90_4]$ specimens have no break stress since their stress-strain behavior is linear-to-failure. The average fracture stresses are listed in Table 3.

Table 2 Break stresses as determined from monotonic tests

θ, °	Average break stress, MPa	C.V., %
0	375	18.2
5	233	41.5
10	171	38.2
15	181	21.8
20	665	4.4
25	157	47.2
30	136	12.4
35	89	13.6
40	66	26.5
45	46	17.3
50	55	8.2
55	58	4.0
60	65	11.0
75	—	—
90	—	—

Table 3 Experimental fracture stresses for all tests

	Monotonic tests		Hysteresis and cyclic tests	
θ, °	Average fracture stress, MPa	C.V., %	Average fracture stress, MPa	C.V., %
0	1770	7.7	1610	10.2
5	1205	4.3	1210	12.8
10	1012	7.1	939	8.1
15	838	1.9	828	3.8
20	723	7.4	713	4.9
25	608	6.1	605	6.8
30	514	8.4	506	5.7
35	421	2.5	429	3.9
40	284	14.8	268	3.6
45	159	13.1	165	9.3
50	104	2.1	115	2.0
55	91	3.9	92	7.7
60	75	2.9	a	
75	38	8.4	a	
90	54	4.6	a	

[a] Hysteresis and cyclic tests not conducted on this laminate.

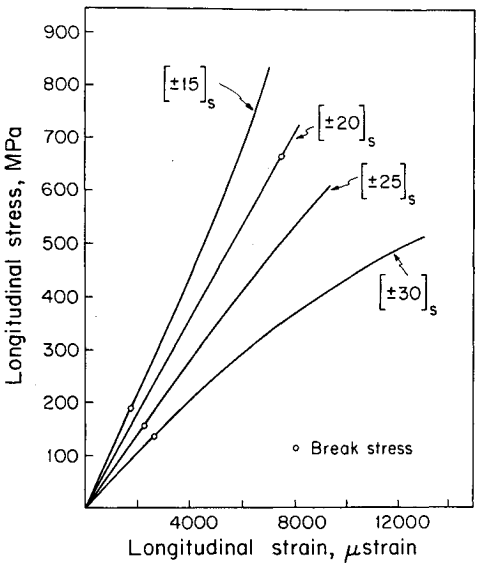

Fig. 4 Typical stress-strain behavior for $\theta = 15°$, 20°, 25°, and 30°.

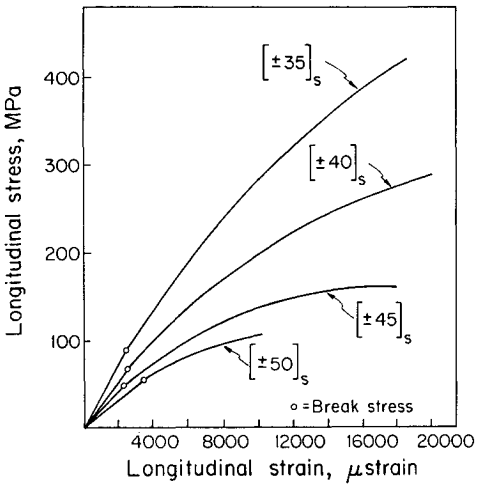

Fig. 5 Typical stress-strain behavior for $\theta = 35°$, 40°, 45°, and 50°.

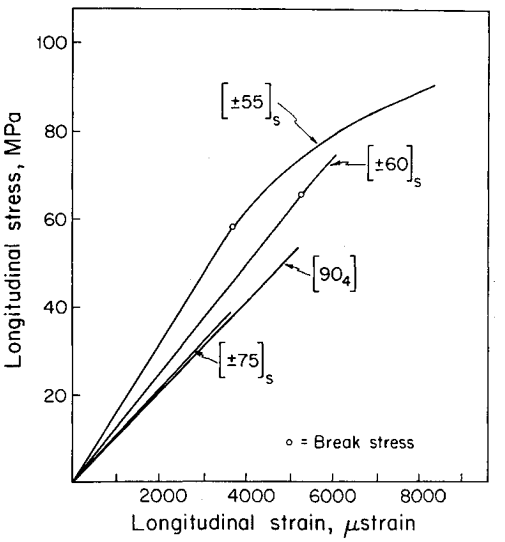

Fig. 6 Typical stress-strain behavior for $\theta = 55°$, 60°, 75°, and 90°.

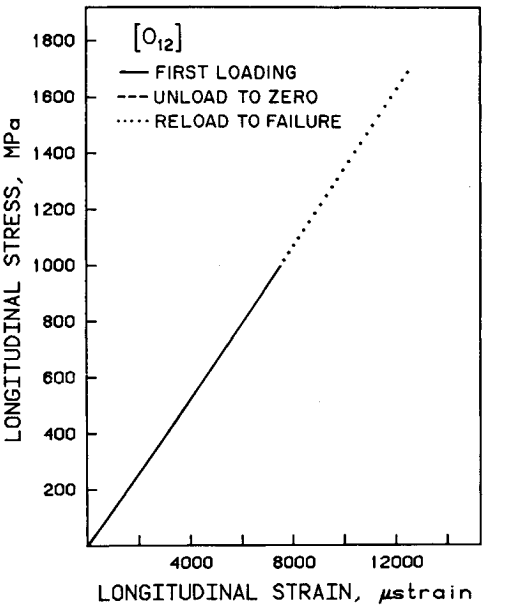

Fig. 7 Typical $[\theta_{12}]$ stress-strain behavior for load, unload, reload-to-failure cycle.

The average measured initial and final longitudinal moduli are reported in Table 4 along with percentage change in modulus from beginning to end of test. The initial longitudinal modulus is compared to that predicted using classical laminated plate theory and the basic unidirectional ply elastic constants for Hercules AS1/3501-6 of $E_L = 130$ GPa, $E_T = 10.5$ GPa, $G_{LT} = 6.0$ GPa, and $\nu_{LT} = 0.28$, where L = fiber direction and T = transverse direction. The experimentally determined initial longitudinal moduli agree well with the predicted values.

The nonlinear stress-strain behavior of these laminates can be classified into two groups: "stiffening," in which the final tangent modulus is larger than the initial modulus; and "softening," in which the final tangent modulus is less than the initial modulus. The results show that for $\theta = 0°$, there is a slight stiffening, on the order of 10%, of the laminate. The amount of stiffening decreases with increasing lamination angle until there is virtually a linear-to-failure behavior for the $[\pm 20]_s$ specimens. From this point on, softening is observed. The amount of softening peaks for $\theta = 45°$. For these $[\pm\theta]_s$ laminates, the tangent modulus actually goes slightly negative just prior to failure, representing a loss in modulus greater than 100%. There is a decrease in the amount of tangent modulus loss, with further increase in lamination angle to the point at which there is linear-to-failure behavior for $\theta = 75°$ and 90°.

Hysteresis and Cyclic Tests

Stress-strain plots of the complete load, unload, load-to-failure hystersis tests are shown in Figs. 7-9 for the $[0_{12}]$, $[\pm 30]_s$, and $[\pm 50]_s$ laminates, respectively. These plots show several important results and are representative of the behavior found in all specimens of all lamination angles. For laminates that stiffen ($\theta = 0°$, 5°, 10°, and 15°), the unload path follows the original load path, leaving no "permanent strain" when all load has been removed. Upon reloading, the stress-strain curve follows the same path as for the original loading and in fact follows the same path to failure as for a specimen loaded monotonically to failure. This can be seen by contrasting the stress-strain curve for the $[0_{12}]$ specimen loaded monotonically to failure in Fig. 3 with that of Fig. 7, which is a similar specimen subjected to a load, unload, reload-to-failure history. This point is further emphasized in the results summarized in Tables 3 and 4. In Table 3, which contains the fracture stresses for these tests, it can be clearly

seen that there is no significant variation in fracture stress between the specimens loaded directly to failure vs those with the load, unload, load-to-failure history. This is true even for the specimens that underwent the 100 load-unload cycles before being loaded to failure. Similarly, the results summarized in Table 4 show that the initial moduli are the same for the various test types and that the final tangent moduli are also the same, regardless of the test type. In Table 4, the initial modulus for the hysteresis and cyclic tests is the modulus measured in the load-to-failure portion of the test.

For the laminates that soften ($\theta > 20°$), similar results are found. The main difference in the hysteresis tests between the laminates that stiffen and those that soften is that for the latter, the unload stress-strain curve does not follow the original stress-strain curve but shows a decided hysteresis effect. Furthermore, the measured strain does not return to zero upon unloading to zero load, but a "permanent strain" remains. These permanent strains were measured approximately five minutes after the load was removed and the specimen ungripped. The strain at the instance of ungripping decreased slightly to these "permanent" values after several minutes. The averages of these measured permanent strains are summarized in Table 5 for the specimens that exhibited significant permanent strains ($> \pm 50$ microstrain). As expected, the amount of permanent strain increases the further the initial loading traversed into the nonlinear region. However, the largest permanent strain occurred for $\theta = 35°$, which was not the laminate that showed the largest percentage reduction in tangent modulus.

Upon reloading to failure, the specimens that soften exhibit a stress-strain curve with the same initial modulus as for the specimens loaded monotonically to failure as shown in Table 4. Upon further loading, the stress-strain curve rejoins the original stress-strain curve at the point to which the specimen was originally loaded. This can be seen by comparing the stress-strain curve for the $[\pm 30]_s$ specimen loaded monotonically to failure in Fig. 4 with that of a similar specimen that underwent a load, unload, reload-to-failure cycle in Fig. 8. This can also be seen for the $[\pm 50]_s$ specimen in Figs. 5 and 9. Thus, just as for the specimens that stiffen, the initial modulus is the same, the final modulus is the same, and the fracture stress is the same (as shown in Table 3), regardless of the test type. It is important to note that no cyclic tests (types G and H) were conducted on laminates that exhibit softening.

Discussion

For the laminates in this investigation, there appear to be two main contributions to the laminate stress-strain nonlinearity: the stiffening nonlinearity in longitudinal tension, and the softening due to shear in the unidirectional ply. Most authors consider the latter but not the former. Some researchers[1,14,15] have noticed this slight stiffening, on the order of 10% for longitudinal tension, which is in line with the 11 to 13% increase in modulus measured for the $[0_{12}]$ specimens

Table 4 Predicted and measured initial longitudinal moduli and final tangent moduli for all tests

		Monotonic tests					Hysteresis and cyclic tests				
θ, °	Predicted initial modulus, GPa	Average measured initial modulus, GPa	C.V., %	Average tangent modulus at failure, GPa	Average percent change in modulus	C.V., %	Average measured initial modulus, GPa	C.V., %	Average tangent modulus at failure, GPa	Average percent change in modulus	C.V., %
0	130	131	2.5	144	+11	6.8	124	3.9	140	+13	5.6
5	128	129	2.2	143	+11	12.6	126	3.9	140	+11	24.4
10	120	119	2.6	131	+9	19.8	117	3.1	126	+8	34.2
15	107	104	2.5	110	+6	32.3	105	4.1	111	+6	23.4
20	89.3	88.0	3.7	82.4	−6	68.2	87.5	3.1	84.0	−4	126.5
25	69.2	67.1	4.6	51.7	−23	16.1	67.6	4.6	50.6	−25	13.9
30	51.0	50.5	2.4	30.2	−40	3.6	49.6	4.1	28.8	−42	8.4
35	36.9	36.1	7.7	9.9	−73	4.9	35.2	3.8	10.6	−70	5.8
40	27.0	27.1	13.0	5.8	−79	10.0	26.1	4.9	4.5	−83	14.3
45	20.6	21.1	9.8	−1.2	−105	34.6	19.3	7.9	−0.4	−102	30.4
50	16.6	15.2	3.5	5.5	−64	33.2	16.0	10.8	5.5	−66	25.9
55	14.1	13.4	5.7	8.9	−34	31.1	13.5	4.4	8.9	−34	17.8
60	12.6	12.4	5.9	10.9	−12	90.1	a				
75	10.8	11.0	9.6	11.0	0	—	a				
90	10.5	11.0	16.9	11.0	0	—	a				

[a] Hysteresis and cyclic tests not conducted on this laminate.

Table 5 Measured permanent strains for hysteresis tests[a,b]

	Test type B		Test type D		Test type F	
θ, °	Average permanent strain, μ strain	C.V., %	Average permanent strain, μ strain	C.V., %	Average permanent strain, μ strain	C.V., %
25	c		140	28.1	c	
30	221	27.7	452	11.0	741	10.0
35	307	13.3	875	13.3	2028	17.6
40	c		610	22.0	c	
45	122	13.5	308	7.3	760	24.5

[a] Hysteresis tests not conducted for $\theta = 60°, 75°, 90°$.
[b] Indicated permanent strain negligible ($< \pm 50$ μ strain), with large variations for $\theta = 0°, 5°, 10°, 15°, 20°, 50°, 55°$.
[c] Test type not conducted on this laminate.

here. Thus, these two basic unidirectional ply stress-strain nonlinearities "compete" to control the overall laminate behavior. For the $[\pm\theta]_s$ laminates, small values of lamination angle result in an overall stiffening behavior; while for larger values, the shear effect is dominant and softening occurs. At $\theta \cong 20°$, the two effects cancel out, resulting in a linear-to-failure stress-strain behavior. The amount of softening peaks at 45° with a complete loss of modulus. This is in line with the fact that the $[\pm 45]_s$ specimens have the largest shear contribution due to a longitudinal load, whereas longitudinal tension and transverse tension are more important contributions for other values of lamination angle.

It is important to note that only three of the five basic loading conditions of the unidirectional ply were measured here: longitudinal tension (stiffening), transverse tension (linear), and shear (softening). The effect of longitudinal compression and transverse compression were not considered. However, compressive stresses in ply axes for all laminates are relatively low and are most likely in the linear stress-strain region, as measured in previous work.

The phenomenon of permanent strain exhibited in the laminates that show significant softening is important. Under repeated loads, permanent strain may accumulate. If this strain becomes large compared to ultimate strain, failure may occur at a reduced stress. No cyclic tests were conducted on laminates that soften, but it is recommended that such tests be performed in order to ascertain the effects that this phenomenon has under repeated loading.

The measured permanent strains indicate that the largest values occur for the $[\pm 35]_s$ laminate. This is somewhat misleading. The original point to which the specimens were loaded prior to unloading was determined on the basis of stress. At the three-quarters point, the $[\pm 35]_s$ specimens had a strain of approximately 13500 μ strain while the $[\pm 45]_s$ specimens had a strain of 9000 μ strain. Thus, the larger permanent strain that resulted in the $[\pm 35]_s$ specimens can be attributed to the fact that these specimens were actually loaded further into the nonlinear region based on strain. It is suggested that in the future these values be normalized to the shear stress/strain in ply axes since this loading condition is the source of the nonlinearity and permanent strain. (Remember that the stiffening nonlinearity causes no measurable permanent strain.)

The results also show that the $[\pm\theta]_s$ laminates, whether they soften or stiffen, do not exhibit any "memory" of previous loading after being reloaded to the original load point for one load, unload, reload cycle. Likewise, no change in fracture stress is observed for specimens subjected to one load, unload, load-to-failure cycle vs those loaded monotonically to failure. Repeated loading (up to 100 cycles) does not alter this fact for laminates that stiffen, but it is important to note that no cyclic tests were conducted on laminates that soften. From the previous discussion on permanent strain, it would be expected that repeated loading would cause a change in stress-strain behavior and a reduction in failure stress. In the case of laminates that stiffen, no permanent strain is observed (even after 100 cycles); thus, any reduction in strength due to cyclic loading would need to come from fiber degradation mechanisms since the fiber dominates the stress-strain behavior.

The laminates investigated herein are not of practical use in most structural applications. However, these results have

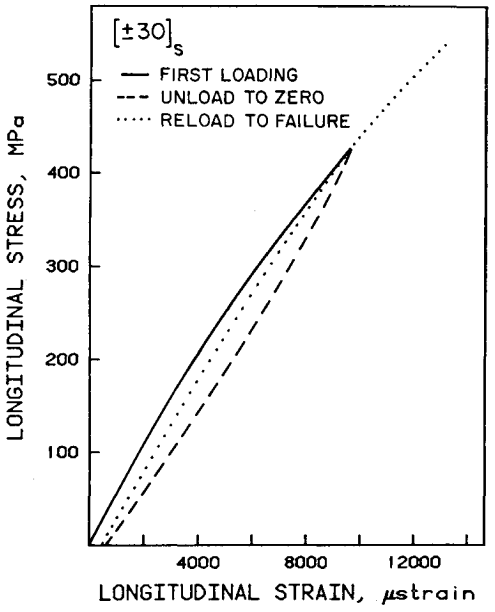

Fig. 8 Typical $[\pm 30]_s$ stress-strain behavior for load, unload, reload-to-failure cycle.

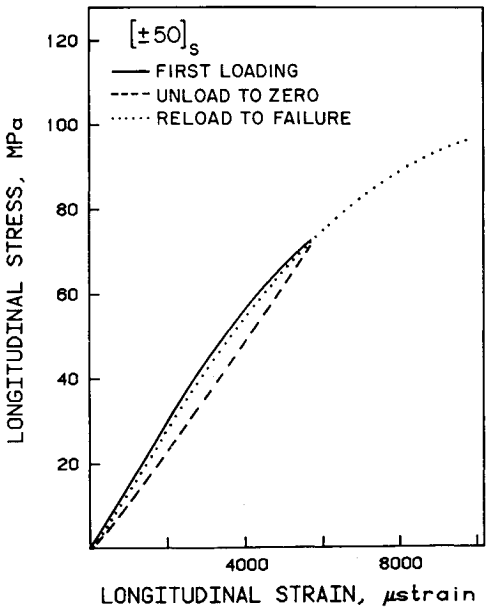

Fig. 9 Typical $[\pm 50]_s$ stress-strain behavior for load, unload, reload-to-failure cycle.

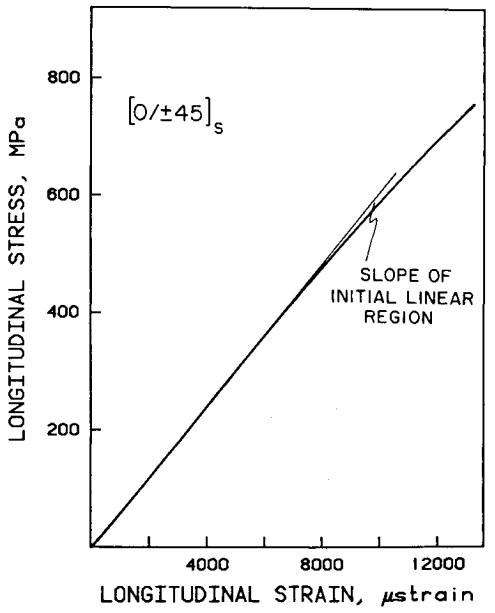

Fig. 10 $[0/\pm 45]_s$ stress-strain behavior (from Ref. 16).

implications for laminates typically used. For example, the stress-strain curve of a $[0/\pm 45]_s$ specimen[16] is shown in Fig. 10. This clearly shows a reduction in tangent modulus of about 10% over the entire curve, with the initial linear region ending at approximately 250 MPa. Stiffening of the 0° plies and softening of the ±45° plies combine to account for this behavior. Although this relatively minor softening may not be important in a monotonic test, permanent strain could accumulate under repeated load, resulting in reduced strength. This would be especially important in the vicinity of stress raisers such as holes, where the material would reach the nonlinear stress-strain region under lower applied loads. It is suggested that similar tests as performed in this investigation (especially cyclic tests) be conducted on specimens with holes and the strains measured at the edge of the hole to determine if there are important permanent strains and related reductions in strength.

Summary

Experimental data have been presented that show nonlinear stress-strain behavior is an important phenomenon in composite laminates. For the graphite/epoxy investigated here, there are two major contributions: stiffening behavior from longitudinal tension and softening due to shear on a unidirectional ply. The load, unload, load-to-failure tests performed point to several important conclusions. First, the load-unload cycle shows a hysteresis effect, with a permanent strain left at zero load for laminates that soften. Second, the reload path has the same initial modulus as the original load path. The reload path then joins the basic stress-strain curve at the point to which the laminate was previously loaded. Third, the laminates show no memory of previous loading after being reloaded to their original load point, as further loading produces a stress-strain curve unaltered by one load, unload, reload cycle. The fracture stress is also unaltered by this previous loading. Nonlinear stress-strain behavior is thus important to consider in design in two particular aspects: 1) stiffness-designed structures will change modulus if the load is above the break point of the material, thus causing changes from expected behavior; and 2) permanent strain may accumulate after many load cycles and alter the ultimate strength of the laminate.

Acknowledgments

The author wishes to thank the undergraduate students who participated in the manufacture and testing of the specimens: David Chin, John Chisholm, Carroll Dodson, Eric Fujii, and David Trop. This work was supported by the Air Force Office of Scientific Research under Grant No. AFOSR-82-0071 and Contract No. F49620-83-K-0015. Dr. Anthony K. Amos was the contract monitor.

References

[1]Sendeckyj, G. P., Richardson, M. D., and Pappas, J. E., "Fracture Behavior of Thornel 300/5208 Graphite/Epoxy Laminate—Part I: Unnotched Laminates," *Composite Reliability*, American Society for Testing and Materials, STP 580, 1973, pp. 528-546.

[2]Petit, P. H. and Waddoups, M. E., "A Method for Predicting the Nonlinear Behavior of Laminated Composites," *Journal of Composite Materials*, Vol. 3, Jan. 1969, pp. 2-19.

[3]Hahn, H. T. and Tsai, S. W., "Nonlinear Elastic Behavior of Unidirectional Composite Laminae," *Journal of Composite Materials*, Vol. 7, Jan. 1973, pp. 102-118.

[4]Hahn, H. T., "Nonlinear Behavior of Laminated Composites," *Journal of Composite Materials*, Vol. 7, April 1973, pp. 257-271.

[5]Amijima, S. and Adachi, T., "Nonlinear Stress-Strain Response of Laminated Composites," *Journal of Composite Materials*, Vol. 13, July 1979, pp. 206-218.

[6]Foye, R. L., "Theoretical Post-Yielding Behavior of Composite Laminates Part I—Inelastic Micromechanics," *Journal of Composite Materials*, Vol. 7, April 1973, pp. 178-193.

[7]Foye, R. L., "Theoretical Post-Yielding Behavior of Composite Laminates, Part II—Inelastic Macromechanics," *Journal of Composite Materials*, Vol. 7, July 1973, pp. 310-319.

[8]Sandhu, R. S., "Nonlinear Response of Unidirectional and Angle Ply Laminates," AIAA Paper 74-380, 1974.

[9]Chin, K. D., "Ultimate Strengths of Laminated Composite Laminates After Initial Failures," *Journal of Composite Materials*, Vol. 3, July 1969, pp. 578-582.

[10]Hahn, H. T. and Tsai, S. W., "On the Behavior of Composite Laminates After Initial Failures," *Journal of Composite Materials*, Vol. 8, July 1974, pp. 288-305.

[11]Chou, S. C., Orringer, O., and Rainey, J. H., "Post-Failure Behavior of Laminates I—No Stress Concentration," *Journal of Composite Materials*, Vol. 10, Oct. 1976, pp. 371-381.

[12]Lagace, P. A., "Delamination Fracture under Tensile Loading," *Proceedings of the Sixth Conference on Fibrous Composites in Structural Design*, Army Materials and Mechanics Research Center, Watertown, MA, AMMRC MS 83-2, 1983.

[13]Vizzini, A. J. and Lagace, P. A., "TELAC Software Manual," Technology Laboratory for Advanced Composites, Masachussets Institute of Technology, Cambridge, in preparation.

[14]Daniel, I. M., Hamilton, W. G., and LaBedz, R. H., "Strain Rate Characterization of Unidirectional Graphite/Epoxy Composite," *Composite Materials: Testing and Design (Sixth Conference)*, American Society for Testing and Materials, STP 787, 1982, pp. 393-413.

[15]Lifshitz, J. M., "Strain Rate, Temperature, and Humidity Influence on Strength and Moduli of a Graphite/Epoxy Composite," *Composites Technology Review*, Vol. 4, No. 1, Spring 1982, pp. 14-19.

[16]Lagace, P. A., "Static Tensile Fracture of Graphite/Epoxy," Ph.D. Thesis, Technology Laboratory for Advanced Composites Report 82-4, Massachusetts Institute of Technology, Cambridge, April 1982.